Inelastic collapse in simple shear flow of a granular medium

M. Alam and C. M. Hrenya*
Department of Chemical Engineering, University of Colorado, Boulder, Colorado 80309
(Received 13 December 2000; published 23 May 2001)

Previous investigations have shown that inelastic collapse is a common feature of inelastic, hard-sphere simulations of *nondriven* (or unforced) flows, provided that the coefficient of restitution is small enough. The focus of the current effort is on a *driven* system, namely, simple shear flow. Two-dimensional, hard-sphere simulations have been carried out over a considerable range of restitution coefficients (r), solids fractions (ν), and numbers of particles (N). The results indicate that inelastic collapse is an integral feature of the sheared system. Similar to nondriven systems, this phenomenon is characterized by a string of particles engaging in numerous, repeated collisions just prior to collapse. The collapsed string is typically oriented along a 135° angle from the streamwise direction. Inelastic collapse is also found to be more likely in systems with lower r, higher ν, and higher N, as is true for unforced systems. Nonetheless, an examination of the boundary between the collapsed and noncollapsed states reveals that the sheared system is generally more ''resistant'' to inelastic collapse than its nondriven counterpart. Furthermore, a dimensionless number V^* is identified that represents the magnitude of the *initial* fluctuating velocities relative to that of a characteristic steady-state velocity (i.e., the product of shear rate and particle diameter). For values of $V^* \gg O(1)$, the *transient* portion of the simulation is found to be more reminiscent of a nondriven system (i.e., isotropic particle bunching is observed instead of diagonal particle bands).

DOI: 10.1103/PhysRevE.63.061308 PACS number(s): 45.70.−n, 45.05.+x, 81.05.Rm, 83.80.Fg

I. INTRODUCTION

Due to their inelastic nature, granular materials display a host of flow phenomena that is not observed in their perfectly elastic counterparts (e.g., molecular gas) [1]. One such phenomenon that has been observed in both ''molecular-dynamic'' simulations and theoretical treatments of granular materials is inelastic collapse [2–6]. Inelastic collapse refers to the state in which a group of particles undergoes an infinite number of collisions in a finite period of time. As a result, the group of particles comes into contact without any attractive forces between the particles.

The physical significance of the collapsed state is not well understood (for recent review, see [7]). Because inelastic collapse is only found to occur when the system is represented as a collection of inelastic hard spheres, collapse is viewed by some as a shortcoming of the hard-sphere model with little, if any, bearing on real granular materials. (A behavior similar to collapse has been observed, however, for an *elastic* hard-sphere system that includes the effects of hydrodynamic lubrication [8]). Accordingly, several modifications to the hard-sphere model that preclude the onset of collapse have been proposed, including the addition of rotational or translational energy prior to the collapsed state, the incorporation of a velocity-dependent coefficient of restitution, and the reduction of energy dissipation during multiparticle contacts (for recent summary, see [9]). Alternatively, another viewpoint holds that collapse signals the onset of long-range velocity and position correlations, which may significantly impact the hydrodynamic behavior of the material. Furthermore, a ''collapsed-like'' state has been observed in experiments involving vertically vibrated beds of particles [10,11] . More specifically, within a range of relatively low vibration amplitudes, a region of motionless particles in constant contact was observed and was found to be surrounded by a less dense collection of fast-moving particles.

Regardless of the physical significance of the inelastic collapse, however, the identification of the range of parameters over which collapse occurs remains an important task. At the very least, this task will lead to the parameter space over which the hard-sphere model is an inadequate representation of a granular material. On the other hand, it may help to identify a region in which additional fluid-mechanical correlations become important and must be accounted for in continuum models.

Much of the previous work on inelastic collapse has focused on *nondriven* or cooling systems (i.e., systems with no energy input). The focus of early efforts was on one-dimensional cooling systems, which were examined from both a theoretical and numerical (i.e., molecular-dynamic simulations) standpoint [2,3,5]. These studies revealed that a critical coefficient of restitution, r^*, exists in which a system will experience inelastic collapse for values of $r < r^*$. This value of r^* was found to increase with the number of particles N contained in the system (i.e., collapse is more likely to occur in systems with higher N). Inelastic collapse has also been observed in the simulations of two-dimensional cooling systems performed by McNamara and Young [4,12]. In these systems, r^* was found to increase with N and ν, where ν represents the area fraction occupied by the particles. The particles taking part in the collapse form a roughly linear string; this behavior is consistent with the theoretical analysis of a three-particle system by Zhou and Kadanoff [6], which indicated that collapse is preferred when the angle between the particles' line of center is small.

Relatively little attention has been given to the occurrence

*Author to whom correspondence should be addressed. Email address: hrenya@colorado.edu

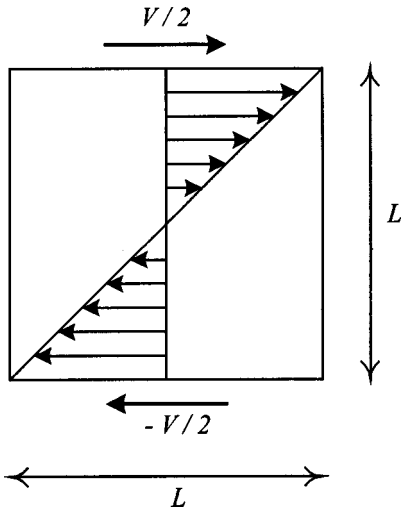

FIG. 1. Simple shear flow system.

of inelastic collapse in *driven* systems (i.e., systems into which energy is continually added). Intuitively, one may expect that collapse would be avoided in such systems due to the presence of associated stresses, which tend to continuously disrupt particle groupings. For the case of a single, randomly forced particle, however, Cornell, Swift, and Bray [13] have shown that collapse occurs in a one-dimensional system where the particle engages in inelastic collisions with the two boundaries.

The current effort provides further evidence of the existence of inelastic collapse in driven systems. The system under examination is two-dimensional, simple shear flow. Unlike the Cornell, Swift, and Bray study [13], energy is supplied to the system via the system boundaries rather than through random particle accelerations. Inelastic hard-sphere simulations of this system were carried out over a range of N, ν, and r, and the results indicate that inelastic collapse is a robust feature of simple shear flow. In particular, similar to nondriven systems, the particles involved in the collapse form a nearly linear configuration and r^* is found to increase with both solids fraction and number of particles (i.e., collapse is more likely to occur at higher values of ν and N). The specific value of r^* (for a given N and ν), however, is generally lower than that of the analogous nondriven system, which thereby indicates that the presence of shear forcing hinders the onset of inelastic collapse. In addition, the final configuration of the collapsed particles typically occurs along an axis at about 135° from the streamwise direction. Finally, for systems with relatively high values of *initial* fluctuating velocities (as compared to the product of the shear rate and particle diameter), the system is observed to experience a *transient* phase in which the particle arrangement bears a greater resemblance to a homogeneous cooling system than that of a sheared system.

II. SIMULATION DESCRIPTION

As illustrated in Fig. 1, the flow regime under consideration is two-dimensional simple shear flow in the x direction. The flow domain is an $L\times L$ square, with the top boundary moving at velocity $V/2$ and the bottom boundary moving at velocity $-V/2$. Accordingly, the system is characterized by the uniform shear rate $\gamma=V/L$. The particles contained in the system are smooth, inelastic disks of uniform size and density. Collisions between particles are assumed to be both instantaneous and binary in nature. Because no external or interparticle forces are present, the particles follow straight-line trajectories between collisions and maintain a constant velocity.

A. Numerical algorithm

In order to track the position and velocity of all particles as a function of time, simulations are carried out using a hard-sphere model for collisions and an event-driven strategy between collisions. In particular, the relationship between the post- and pre-collisional velocities of the two particles is dictated by the hard-sphere model

$$\mathbf{v}_{1,\mathrm{post}}=\mathbf{v}_{1,\mathrm{pre}}-\tfrac{1}{2}(1+r)[\mathbf{k}\cdot(\mathbf{v}_{1,\mathrm{pre}}-\mathbf{v}_{2,\mathrm{pre}})]\mathbf{k} \tag{1}$$

$$\mathbf{v}^*_{2,\mathrm{post}}=\mathbf{v}_{2,\mathrm{pre}}+\tfrac{1}{2}(1+r)[\mathbf{k}\cdot(\mathbf{v}_{1,\mathrm{pre}}-\mathbf{v}_{2,\mathrm{pre}})]\mathbf{k}, \tag{2}$$

where the subscripts 1 and 2 refer to particles 1 and 2, respectively; $\mathbf{v}_{\mathrm{pre}}$ refers to the precollisional velocity, $\mathbf{v}_{\mathrm{post}}$ refers to the postcollisional velocity, r is the coefficient of restitution, and $\mathbf{k}$ is the unit vector pointing from the center of particle 1 to the center of particle 2. In order to proceed from one collision to the next, a search of all upcoming collisions, and the time required for the collisions to occur, is made. Once the collision pair with the shortest time to the next collision is identified, the system is advanced by that amount of time, and the collision is resolved according to equation (1) and (2). This ''event-driven'' strategy is made efficient using the link-cell algorithm to search for future collisions [14].

To achieve the state of simple shear flow, a Lees-Edwards boundary condition [15] is implemented at the top and bottom boundaries. This condition, which is periodic in the y direction, accounts for the momentum transfer arising from the imposed shear field. More specifically, a particle that leaves the domain through the top (or bottom) boundary returns to the domain through the bottom (or top) boundary with a streamwise velocity component that has been adjusted according to its new location in the flow field. The right and left boundaries are also periodic, though particles that leave through one of these boundaries are returned to the domain at the opposite boundary with the same velocity.

The simulation is initialized by positioning particles on a nearly square lattice, with small random displacements in both the x and y directions. The velocity of each particle is initially set to its mean horizontal component (based on its vertical location in the shear field), plus a small random component in both directions. The simulation then proceeds from collision to collision (as described above) until collapse occurs or the maximum number of collisions is reached; the details of collapse detection are presented in the following section.

The inputs required for simulation include the particle mass m, d, L, γ, ν, and r. Recall that V is determined by the relation $\gamma = V/L$ and N is set according to the definition of solids area fraction:

$$\nu = \frac{N(\pi d^2/4)}{L^2}. \tag{3}$$

Hence, the dimensionless parameters that characterize the system include d/L, ν, and r, or the equivalent set N, ν, and r [based on relation shown in (3)]. For the current effort, N, ν, and r are chosen as the independent control parameters, and m, L, and γ are each set to unity. The specific parameter space under consideration includes $N = 25-2500$, $\nu = 0.1-0.5$, and $r = 0.01-0.99$.

For purposes of validation, results from the current simulation were compared with those obtained in previous investigations. In particular, the dimensionless stresses were shown to agree well with those previously obtained for a simple shear flow system [16], and the onset of collapse was found to agree with that previously obtained for a homogeneous cooling system ($\gamma = 0$) [4,12].

B. Detection of inelastic collapse

As described above, inelastic collapse refers to the condition in which a collection of particles undergoes an infinite number of collisions in a finite period of time. Because such a state cannot be resolved numerically, the onset of collapse in discrete-particle simulations is identified by a sequence of collisions with continually decreasing time and space scales. Once these scales decrease enough such that the limit of machine precision is reached, the simulation is halted and collapse is said to have occurred.

The specific criterion used for collapse detection in this work is based on that put forth by McNamara and Young [12] in their study of homogeneous cooling systems. Namely, inelastic collapse is identified by tracking the separation distance d_{sep} between particles. The separation distance, which is evaluated at the time of collision, refers to the distance between the two particles involved in the upcoming collision. Once d_{sep}/d drops below the limit of machine precision, which is 10^{-16} in this case, the simulation is stopped. This behavior is illustrated in Fig. 2, which shows the results for a simulation with $N = 500$, $\nu = 0.3$, and $r = 0.4$. As is evident from this plot, the normalized separation distance remains relatively constant for approximately 270 300 collisions, and then experiences a continual decrease (spanning approximately 12 orders of magnitude). At $C = 270\,505$, machine precision is reached and the system has collapsed.

For the purposes of the current work, a simulation is allowed to proceed until collapse is detected or until the number of collisions per particle, C/N, reaches 6000, whichever happens first. This (arbitrary) choice of the maximum allowable C/N *does* influence whether a system is considered collapsed or not (i.e., it is possible that collapse may be observed in a system at $C/N > 6000$). The C/N limit used here, however, is chosen to ensure that each system examined reaches a statistical steady state, and that this steady state occurs over the majority of the simulated time period. To determine if a system has reached a steady state, the quantity $\langle v'^2 \rangle$ is monitored, where $\mathbf{v}'$ is the fluctuating component of the particle velocity (relative to its position in the shear field) and $\langle\ \rangle$ denotes an average taken over all particles in the system. For the parameter space considered in this study, $\langle v'^2 \rangle$ typically reaches a statistically steady value at $C/N \leqslant 200$. (Note that the higher-order moment of the fluctuation velocity, namely, $\langle v'^4 \rangle / \langle v'^2 \rangle^2$ was also monitored, and was found to achieve a steady state prior to its lower-order counterpart.)

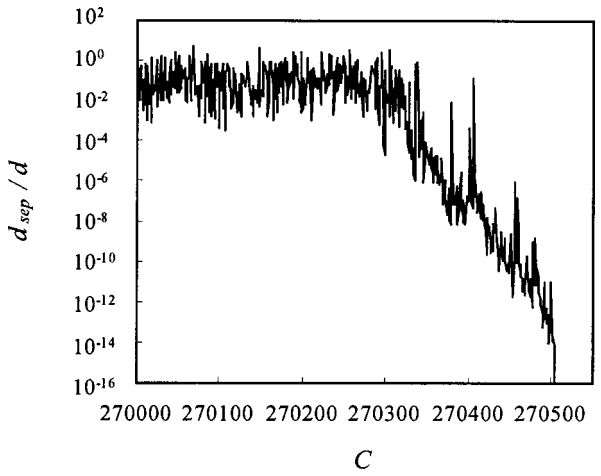

FIG. 2. Normalized separation distance as a function of number of collisions for a simulation with $N = 500$, $\nu = 0.3$ and $r = 0.4$.

III. RESULTS AND DISCUSSION

The hard-sphere simulations of the simple shear system were carried out over the parameter space $N = 25-2500$, $\nu = 0.1-0.5$, and $r = 0.01-0.99$. In the following sections, the qualitative and quantitative nature of the simulation results are presented and discussed.

A. Characteristics of the noncollapsed and collapsed states

Figure 3 depicts the final particle positions for a series of simulations with $N = 500$, $\nu = 0.3$, and various values of the restitution coefficient. The simulations for other N and ν display similar characteristics, and thus will not be presented for the sake of brevity.

As has been found in the previous investigations of inelastic collapse, the onset of collapse is strongly influenced by the coefficient of restitution. For the higher values of r shown in subplots (a)–(c), the simulations reach the maximum number of collisions (i.e., $C/N = 6000$) without experiencing collapse. As detailed in subplots (d)–(f), however, lower r values give rise to a collapsed state before the maximum number of collisions is reached (i.e., $C/N < 6000$). Furthermore, inelastic collapse is observed to take place more quickly as the coefficient of restitution is lowered. For example, collapse is found to occur at $C/N = 541$ for $r = 0.40$ and at $C/N = 0.114$ for $r = 0.01$.

Another feature that is portrayed by the snapshots contained in Fig. 3 concerns the grouping of particles involved

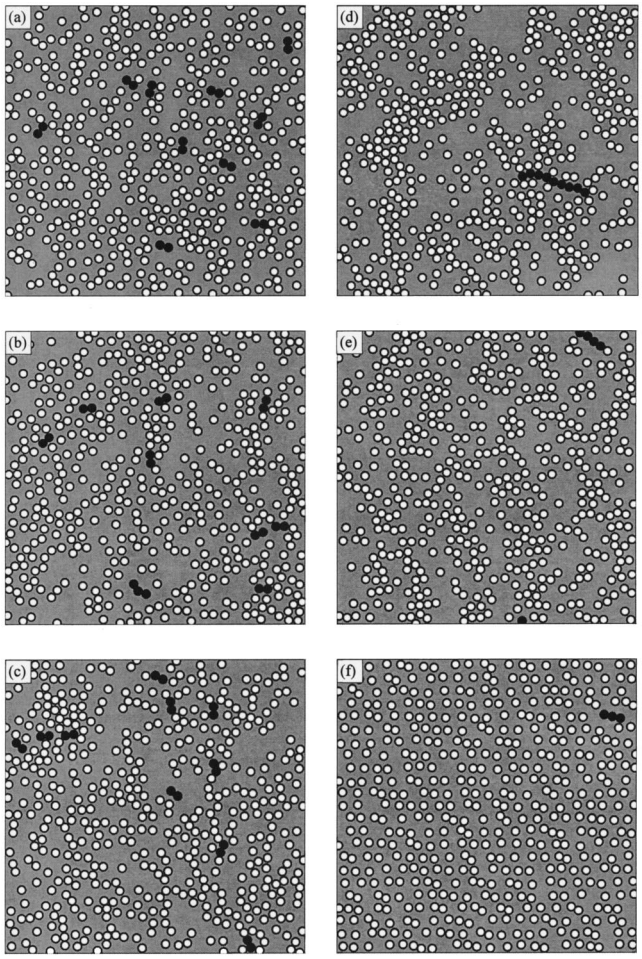

FIG. 3. Final particle configurations for simulations with $N=500$, $\nu=0.3$, and various r: (a) $r=0.99$, $C/N=6000$, last ten collisions in black; (b) $r=0.80$, $C/N=6000$, last ten collisions in black; (c) $r=0.60$, $C/N=6000$, last ten collisions in black; (d) $r=0.40$, $C/N=541.01$, last 99 collisions in black; (e) $r=0.20$, $C/N=2.162$, last 35 collisions in black; (f) $r=0.01$: $C/N=0.114$, last seven collisions in black.

in the collapse. In order to discern such behavior, the particles involved in the collisions just prior to the end of the simulations are shaded black. More specifically, for the snapshots of noncollapsed systems [Figs. 3(a)–3(c)], only the particles involved in the last ten collisions are shaded black. For those snapshots representing collapsed systems [Figs. 3(d)–3(f)], the black particles indicate those involved in collisions after which the normalized separation distance did not rise above 10^{-4} (i.e., those particles involved in inelastic collapse). For example, as shown in Fig. 2, $d_{\mathrm{sep}}/d<10^{-4}$ for collisions $C=270\,407$ and beyond; the particles involved in all these collisions are blackened in the corresponding snapshot of Fig. 3(d). As is apparent from subplots (a)–(c) for the noncollapsed systems, the pairs of particles involved in the final ten collisions are spread throughout the flow domain. On the other hand, the collapsed systems pictured in subplots (d)–(f) indicate that the same group of particles undergo repeated collisions with one another at the onset of collapse. For $r=0.4$ [Fig. 3(d)], the last 99 collisions involve only nine particles. As r is decreased further [Figs. 3(e) and 3(f)], collapse involves fewer particles and occurs over a shorter number of collisions (i.e., the decrease in d_{sep}/d occurs more quickly). It is also interesting to note that for each of the systems that displays inelastic collapse, the particles partaking in the collapse are arranged in a roughly linear string. This behavior is consistent with that of the two-dimensional cooling systems investigated by McNamara and Young [4,12]. Unlike the homogenous cooling systems, however, the collapsed string in simple shear flows exhibits a preferred direction. As is evidenced by Fig. 3(d)–3(f) (as well as the other simulations that were performed), the final orientation of the collapsed string is typically oriented along an axis approximately 135° from the flow direction.

The final particle configurations given in Fig. 3 also demonstrate the various flow regimes that occur in the simple shear flow system. Namely, as r is decreased from 0.99 to 0.01, the following flow regimes are encountered: kinetic→clustering→collapse. The kinetic regime, which occurs in the nearly-elastic limit [Fig. 3(a)], is characterized by a fairly homogeneous distribution of particles throughout the domain. As the restitution coefficient is lowered, the particle configuration becomes less random and organized structures or ''clusters'' begin to align along a roughly 45° angle from the streamwise direction [Figs. 3(b) and 3(c)], as was previously observed by Hopkins and Louge [16] and Tan and Goldhirsch [17] for the simple shear system. Finally, as r is decreased further, inelastic collapse is found to occur [Figs. 3(d)–3(f)]. Again, a similar pattern of events is found to take place in the homogeneous cooling systems examined by McNamara and Young [12]. It is also worthwhile to note that when collapse occurs in the system with $r=0.4$, the system has already reached a statistical steady state (which occurs at $C/N\sim 20$ for this set of conditions) and thus the clustering pattern is readily observed. At the lowest restitution coefficient [Fig. 3(f)], however, the system collapses well before a steady state is attained. Accordingly, the final particle positions are much more homogeneous in nature, due to the randomness of their initial configuration.

These results indicate that the qualitative nature of collapse in two-dimensional simple shear flows is similar to that of its nondriven counterpart (i.e., homogenous cooling system). In the following section, the quantitative nature of the collapse phenomenon in simple shear will be presented and compared to the previous work on cooling systems.

B. Boundary between noncollapsed and collapsed regimes

The results presented in Fig. 3 indicate that critical restitution coefficient at which the transition between the noncollapsed and collapsed states appears to have a value in the range $0.4<r^*<0.6$ for $N=500$ and $\nu=0.3$. In order to further refine this value and to determine the ''repeatability'' of the results, a wide range of r values were examined, and simulations with a given value of r were repeated ten times each. Because each instance of a simulation begins using random particle positions and fluctuating velocities, the detailed progression of the simulated system is different for each of the repeated simulations. Hence, for a given value of

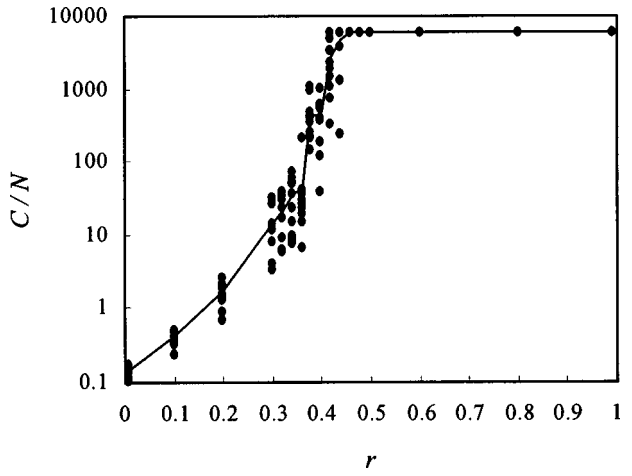

FIG. 4. Variation of total number of collisions (per particle) with r for simulations with $N=500$ and $\nu=0.3$. The data points indicate the results of individual simulations, whereas the line connects the average C/N value obtained for ten simulations at a given r.

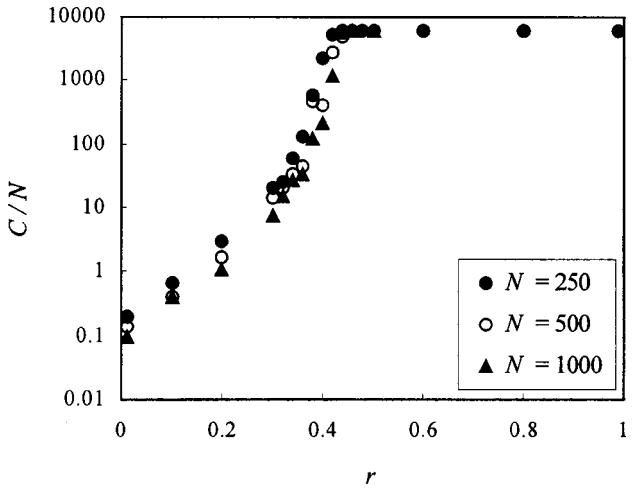

FIG. 5. Dependence of total number of collisions (per particle) on N for system with $\nu=0.3$. Each data point represents average of ten simulations.

r, some simulations may experience collapse, while others may not. The results for the series of simulations with $N=500$ and $\nu=0.3$ are pictured in Fig. 4, which contains the C/N value as a function of r. Results from individual simulations are represented by data points, whereas the line connects the average C/N values for each restitution coefficient investigated. For values of $r\leqslant 0.4$, all simulations are observed to experience collapse before the maximum number of collisions is reached (i.e., $C/N\leqslant 6000$). Furthermore, collapse is seen to occur sooner for systems with lower restitution coefficients. For $r\geqslant 0.46$, none of the simulated systems display inelastic collapse (i.e., $C/N=6000$). In the intermediate range of $0.4<r<0.46$, however, some of the simulations result in collapse while others do not. Accordingly, the critical coefficient of restitution lies within this range. If r^* is defined as the value of r for which at least 50% of the simulations result in a collapsed state [12], then r^* is found to be 0.429 for $N=500$ and $\nu=0.3$. Finally, as was mentioned above, inelastic collapse is observed to occur in systems both before and after a statistical steady state is reached (steady state occurs at $C/N\sim 20$).

In addition to the aforementioned series of simulations performed for $N=500$ and $\nu=0.3$, similar simulations were also performed for other values of N and ν. The resulting dependence of the collapsed state on N and ν is depicted in Figs. 5 and 6, respectively. In these graphs, each data point represents the *average* of ten simulations. As is revealed in Fig. 5, for a fixed coefficient of restitution, the C/N values generally decrease as the number of particles increases. Accordingly, collapse is more likely to occur earlier in systems with higher N values. In a similar manner, Fig. 6 indicates that a larger solids fraction is typically associated with a lower value of C/N, and thus collapse is more probable in systems with a larger value of ν.

Collectively, the results portrayed in Figs. 5 and 6 indicate that the critical coefficient of restitution increases with both N and ν. This information is plotted in Fig. 7 for each combination of N and ν that was examined. The qualitative nature of the dependence of r^* on these two quantities is consistent with previous investigations on two-dimensional homogeneous cooling systems [4,12]. Namely, as N or ν increases, so does r^*. Quantitatively, however, differences are observed. For example, over the range of N investigated, r^* is less sensitive to changes in N than has been previously observed in the nondriven systems. In particular, a linear fit of the current data to r^* vs $\ln(N)$ yields a slope of 0.035 for $\nu=0.5$, whereas a slope of ~ 0.2 was observed at $\nu=0.5$ for homogeneous cooling systems [12].

A more direct comparison between the values of r^* obtained for the simple shear and homogeneous cooling systems is featured in Fig. 8. In this plot, the dependence of the critical restitution coefficient is presented as a function of the dimensionless optical depth:

$$\frac{\lambda}{d}=\frac{\nu L}{d}=\tfrac{1}{2}\sqrt{N\pi\nu}, \tag{4}$$

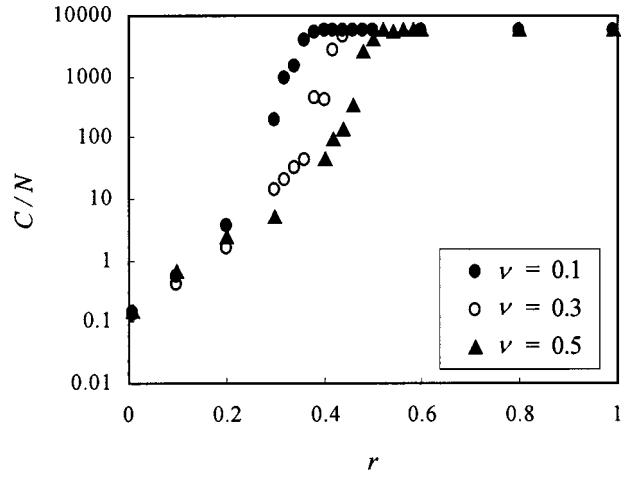

FIG. 6. Dependence of total number of collisions (per particle) on ν for system with $N=500$. Each data point represents average of ten simulations.

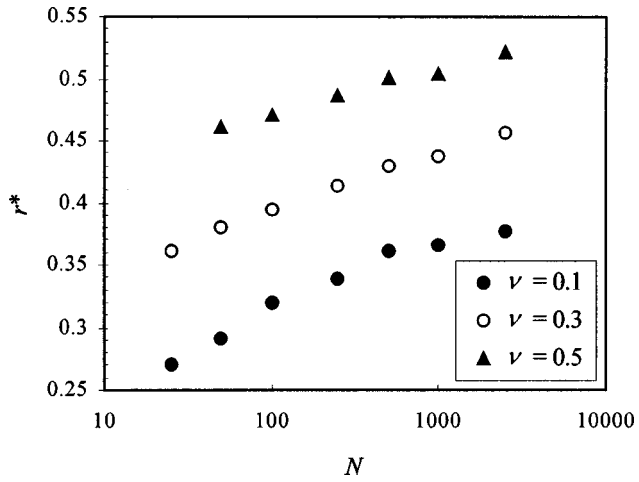

FIG. 7. Dependence of critical coefficient of restitution on both N and ν.

where λ represents the (dimensional) optical depth. Physically, the optical depth represents the distance that a ray of light, while traveling across the width of the domain (L), travels within particles. Equivalently, λ/d is the number of particles contained in a one-dimensional slice through the two-dimensional system. As is apparent from Eq. (4), λ/d combines the effects of both N and ν into a single parameter. For homogenous cooling systems, McNamara and Young [12] found that by considering r^* as a function of λ alone, the data for various (N,ν) combinations approximately collapsed onto a single curve. Furthermore, they found that the data compared well with both the independent collision wave (ICW) model of Bernu and Mazighi [2] and the cushion model (CM) of McNamara and Young [3]. For two-dimensional systems, these models take the following forms:

$$r^*_{\mathrm{ICW}} = \tan^2\left[\frac{\pi}{4}\left(1-\frac{2}{\lambda/d}\right)\right] \tag{5}$$

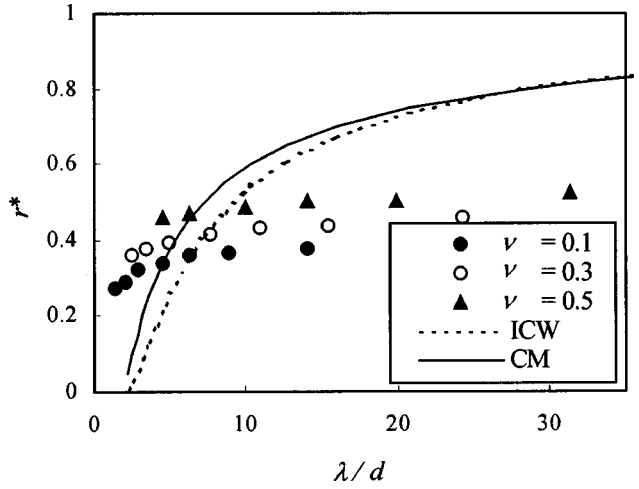

FIG. 8. Dependence of critical restitution coefficients on (dimensionless) optical depth, and comparison of r^* with theoretical predictions.

$$\frac{\lambda}{d} = \frac{\ln[(1-r^*_{\mathrm{CM}})/4]}{\ln[(1+r^*_{\mathrm{CM}})/2]}. \tag{6}$$

[Note that in order to obtain the forms of Eqs. (5) and (6) shown above, two modifications have been made to the original models. First, because the original models were developed based on n particles colliding with a wall, the relation $N=2n$ was substituted in order to instead account for collisions within the interior of the medium. Second, since the models were derived for one-dimensional systems, the quantity N was replaced by λ/d.] As is evident from Fig. 8, the results from the current simulations of simple shear flow do not display the same characteristics as those of their nondriven counterparts. Specifically, the data continue to exhibit a systematic variation according to solids fraction. In addition, the r^* values are not well predicted by either of the models. In particular, the simulation values for $\lambda/d>5$ are generally lower than those predicted by the two theories. Since the nondriven systems have been shown to compare fairly well with the theoretical predictions in this range [12], the current results indicate that driven systems are more ''resistant'' to collapse than the nondriven systems. In other words, the transition between the noncollapsed and collapsed state occurs at a lower coefficient of restitution in the simple shear system as compared to the homogeneous cooling system. For $\lambda/d<5$, the model predictions for r^* are lower than the values obtained via simulation; a similar comparison has also been reported for homogeneous cooling systems [12].

C. Sensitivity of collapse boundary to initial and boundary conditions

As discussed above, all of the aforementioned simulations were carried out using the same initial and boundary conditions. Specifically, the fluctuating component of the velocity field was initially randomly distributed between -10^{-3} and 10^{-3} in each direction (i.e., $-0.001 \leqslant v'_{x0}, v'_{y0} \leqslant 0.001$, where v'_{x0} and v'_{y0} refer to the initial fluctuating velocity components in the streamwise and transverse directions, respectively), and the shear rate was kept constant at 1.0. Together, these two quantities can be used to define a dimensionless number,

$$V^* = \frac{|v'_{x0}, v'_{y0}|_{\max}}{\gamma d}, \tag{7}$$

where the subscript max denotes the maximum value of a given quantity. The relevance of this dimensionless number is demonstrated in Fig. 9 for the case of $N=500$ and $\nu=0.3$. In particular, this figure contains results from a series of four simulations in which V^* remained fixed (at 0.0362) while the initial and boundary conditions ($|v'_{x0},\ v'_{y0}|_{\max}$ and γ) were varied across several orders of magnitude. Again, each data point represents the average C/N values over ten simulations. As is demonstrated in this plot, the C/N dependence on r is observed to fall onto a single curve, thereby indicating the universality of system behavior when V^* is held constant.

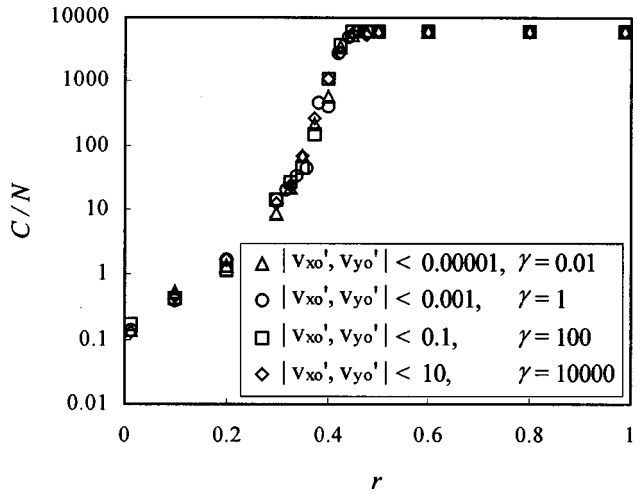

FIG. 9. Simulations for systems with identical values of dimensionless number $V^*(=0.0362)$. Each data point represents average of ten simulations for $N=500$ and $\nu=0.3$.

In order to determine the effect of the magnitude of V^* on the flow behavior, a series of simulations was also performed in which V^* was varied. Figure 10 illustrates this effect for a system with $N=500$, $\nu=0.3$. The various values of V^* represented in this figure were achieved by letting $\gamma=1.0$ and varying the values of $|v'_{x0},v'_{y0}|_{\max}$ accordingly. (Note that the same behavior was also observed when γ was instead varied and $|v'_{x0},v'_{y0}|_{\max}$ was held constant.) As is demonstrated in this plot, the C/N dependence on r is observed to follow one of two trends, depending on the magnitude of the dimensionless number. For high values of V^*, namely, $V^* \gg O(1)$, collapse is observed to occur at fewer collisions in the range $0.3<r<0.6$. A closer examination of these collapsed systems indicates that this behavior occurs in conjunction with a final particle configuration that is similar to the configurations observed in two-dimensional homogeneous cooling systems [4,18]. More specifically, as is exemplified in Fig. 11 for the case of $V^*=3\,620\,000$ and $r=0.4$, particles are observed to have amassed in tightly packed, randomly distributed bunches at the time of collapse. This behavior is in contrast to collapsed systems with lower V^*, which form looser structures aligned along diagonal bands [see Fig. 3(d) for comparison]. Thus, it appears that sheared systems with relatively high values of V^* experience a phase that more closely resembles the behavior associated with a nondriven system (i.e., the large magnitude of the fluctuating velocities initially masks the effects of the shear velocity). Because nondriven systems are less resistant to collapse than their driven counterparts (as discussed above), systems with higher values of V^* are thus more prone to undergo collapse at a fewer number of collisions, as is confirmed by Fig. 10. It is also worthwhile to note that the ''homogeneous cooling'' phase is also experienced by systems that do *not* collapse. Such behavior is exemplified in Fig. 12, which contains two particle snapshots from a simulation with $V^*=3\,620\,000$ and $r=0.6$. At $C/N=100$ [Fig. 12(a)], the system exhibits (isotropic) particle bunching. This pattern is no longer apparent at $C/N=1000$ [Fig. 12(b)]. Instead, a more homogeneous arrangement of particles is observed in this snapshot, as is characteristic of sheared flows. Thus, unlike the dimensionless parameters N, ν, and r that appear to completely characterize the final *steady state* of the system, the dimensionless number indicated by Eq. (7) is also required in order to characterize the *evolution* of the system.

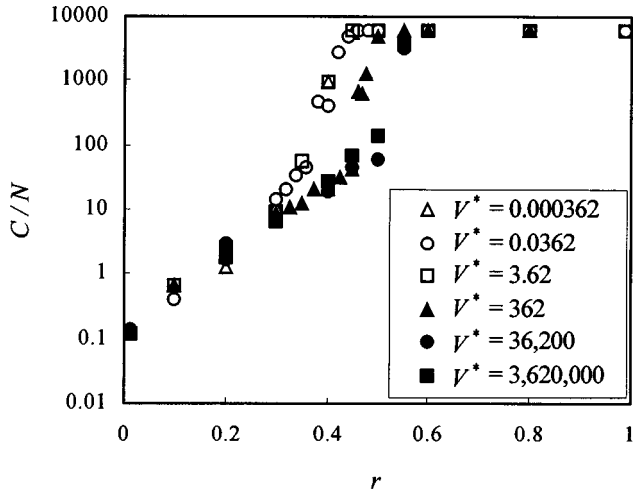

FIG. 10. Effect of dimensionless number V^* on the onset of collapse. Each data point represents average of ten simulations for $N=500$ and $\nu=0.3$.

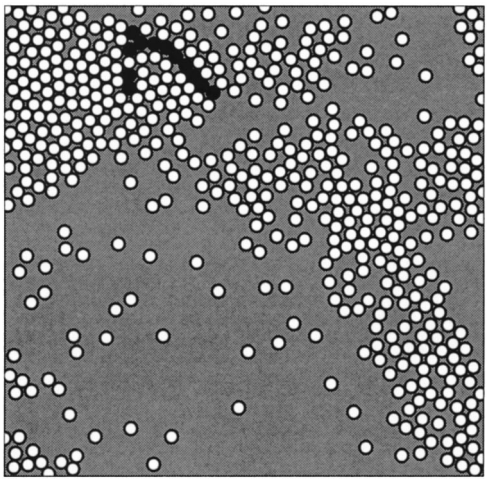

FIG. 11. Final particle configuration for collapsed system with $N=500$, $\nu=0.3$, $V^*=3\,620\,000$ and $r=0.4$; $C/N=32.7$, last 91 collisions in black. [For comparison with system using $V^*=0.0362$, see Fig. 3(d).]

IV. SUMMARY

For this investigation, inelastic hard-sphere simulations of two-dimensional, simple shear flow have been carried out over a considerable range of r, N, and ν. Similar to numerous previous investigations of unforced systems, it has been found that inelastic collapse is an integral feature of the sheared (driven) system. Namely, as r is decreased from unity while N and ν are kept constant, the following flow regimes are observed: kinetic→clustering→collapse. Quali-

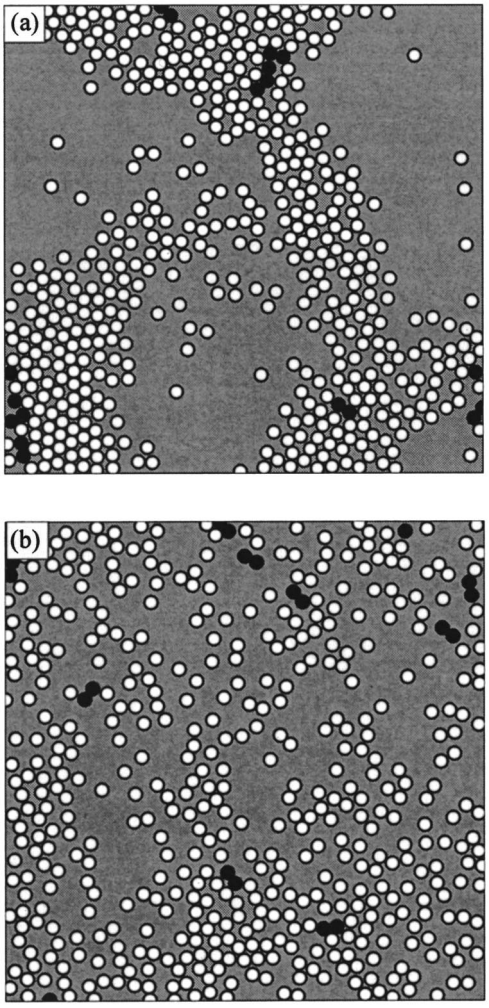

FIG. 12. Particle snapshots for noncollapsed system with $N=500$, $\nu=0.3$, $V^*=3\,620\,000$ and $r=0.6$ at (a) $C/N=100$ and (b) $C/N=1000$; last ten collisions in black.

tatively, the properties of the collapsed state are similar to those observed in the nondriven counterpart (i.e., two-dimensional homogeneous cooling system). The onset of collapse is characterized by a rapid decrease in the separation distance between particles involved in the upcoming collision. In addition, the particles involved in the repeated collisions just prior to collapse are arranged in a roughly linear pattern (though unlike homogeneous cooling systems, the collapsed arrangement in simple shear takes on a preferred direction). Furthermore, the sheared system is found more likely to collapse with an increase in N or ν.

The quantitative nature of inelastic collapse in simple shear systems, however, does differ than that of a homogeneous cooling system. Generally speaking, the coefficient of restitution that demarcates the collapsed and noncollapsed regimes (r^*) is lower than was previously found for nondriven systems, thereby indicating that the onset of collapse is somewhat hampered by the continual input of energy (via shear work). Furthermore, the dependence of r^* on N and ν is not successfully captured using the ''optical depth'' parameter, which combines the effects of both N and ν. Finally, it is also found that evolution of a system with fixed N, ν, and r may be markedly different depending on the value of the dimensionless parameter $V^*=|v'_{x0},v'_{y0}|_{\max}/(\gamma d)$. For $V^*\gg O(1)$, the magnitude of the fluctuating velocity initially conceals the effect of the shear work. As a result, a transient ''homogeneous cooling'' phase (i.e., isotropic particle bunching) is observed prior to the onset of conventional shearing behavior (i.e., particle clusters along diagonal bands).

Because inelastic collapse signals a breakdown in the model used to describe particle-particle collisions (i.e., a binary collision rule is no longer appropriate), the observations of collapse described herein reveal the limitations of using an inelastic, hard-sphere model to describe shear flows. Although several techniques have been shown to eliminate the collapse phenomenon, the physical mechanisms underlying these techniques are not necessarily the same. For example, previous efforts have shown that the incorporation of either a velocity-dependent coefficient of restitution [19] or a reduction in energy loss during multiparticle contacts [9] is capable of preventing inelastic collapse. These two modifications are expected to alter the flow behavior in different manners, though the extent of these differences has not yet been ascertained. Furthermore, the current effort also has implications on kinetic-theory models of granular systems. Specifically, because kinetic-theory treatments are based on the assumption of instantaneous, binary collisions between particles, observations of inelastic collapse can be linked to a violation of this assumption. Again, the effect of such a violation on the ability of kinetic-theory models remains uncertain.

ACKNOWLEDGMENTS

C.M.H. gratefully acknowledges funding support from The Petroleum Research Fund, administered by the American Chemical Society. C.M.H. would also like to extend her thanks to Professor Isaac Goldhirsch for providing his insights during the course of this study, to Professor Rick Clelland for his guidance on code development, and to Steven Dahl for his work on the source code.

[1] H. M. Jaeger, S. R. Nagel, and R. P. Behringer, Phys. Today **49** (4), 32 (1996).
[2] B. Bernu and R. Mazighi, J. Phys. A **23**, 5745 (1990).
[3] S. McNamara and W. R. Young, Phys. Fluids A **4**, 496 (1992).
[4] S. McNamara and W. R. Young, Phys. Rev. E **50**, 28 (1994).
[5] P. Constantin, E. Grossman, and M. Mungan, Physica D **83**, 409 (1995).
[6] T. Zhou and L. P. Kadanoff, Phys. Rev. E **54**, 623 (1996).
[7] L. P. Kadanoff, Rev. Mod. Phys. **71**, 435 (1999).
[8] R. S. Farr, J. R. Melrose, and R. C. Ball, Phys. Rev. E **55**, 7203 (1997).
[9] S. Luding and S. McNamara, Granular Matter **1**, 113 (1998).

[10] J. S. Olafsen and J. S. Urbach, Phys. Rev. Lett. **81**, 4369 (1998).
[11] W. Losert, D. G. W. Cooper, and J. P. Gollub, Phys. Rev. E **59**, 5855 (1999).
[12] S. McNamara and W. R. Young, Phys. Rev. E **53**, 5089 (1996).
[13] S. J. Cornell, M. R. Swift, and A. J. Bray, Phys. Rev. Lett. **81**, 1142 (1998).
[14] M. P. Allen and D. J. Tildesley, *Computer Simulation of Liquids* (Oxford University Press, New York, 1989).
[15] A. W. Lees and S. F. Edwards, J. Phys. C **5**, 1921 (1972).
[16] M. Hopkins and M. Louge, Phys. Fluids A **3**, 47 (1991).
[17] M.-L. Tan and I. Goldhirsch, Phys. Fluids **9**, 856 (1997).
[18] I. Goldhirsch and G. Zanetti, Phys. Rev. Lett. **70**, 1619 (1993).
[19] D. Goldman, M. D. Shattuck, C. Bizon, W. D. McCormick, J. B. Swift, and H. L. Swinney, Phys. Rev. E **57**, 4831 (1998).